



Synthesis of Homogeneously Dispersable Magnetite Nanoparticles via Size Control and Surface Modification for Hyperthermia Application†

EUN-HEE LEE and CHANG-YEOL KIM*

Nano-Convergence Intelligence Material Team, Korea Institute of Ceramic Engineering and Technology, 153-801 Seoul, Republic of Korea

*Corresponding author: E-mail: cykim15@kicet.re.kr

Published online: 10 March 2014;

AJC-14858

Magnetite nanocrystals draw attractions of their applications for hyperthermia therapy in cancer killing by heating. These days, hyperthermia together with chemotherapy shows improved cancer treatment effects. The size control and surface modification of magnetite nanoparticles is very important for the application of biotechnology, because a magnetic property depends upon crystal sizes and a dispersability of magnetite changes with surface chemical state of the particles. We synthesized different-sized magnetite nanoparticles by changing the molar concentration of iron acetylacetonate and oleic acid-capped magnetite shows the hydrophobicity. To confer hydrophilic property, we modified the surface of magnetite nanoparticles with polyethylene glycol. We could present the possibilities of the dispersion of magnetite nanoparticles with different crystal sizes by surface modification with polyethylene glycol within phosphate buffer solution.

Keywords: Magnetite, Hyperthermia, Superparamagnetic, Surface modification, Size control.

INTRODUCTION

Hyperthermia therapy is considered as a promising form of cancer therapy with the well-known methods of surgery, chemotherapy and radiotherapy. There are two kinds of heating treatments: mild hyperthermia is performed between 41 and 46 °C to stimulate the immune response for non-specific immunotherapy of cancers and thermoablation at more than 46 °C up to 56 °C¹. In the past, external means of heat delivery were used such as ultrasonic or microwave treatments, but recently research has focused on the injection of magnetic fluids²⁻⁴. When a magnetic fluid is subjected to an alternating magnetic field, the particles become powerful heat sources, destroying tumor cell. The particles are preferably suspensions of superparamagnetic particles. The use of iron oxides in tumor heating was first proposed by Gilchrist *et al.*⁵. They investigated the hyperthermia effect of 20-100 nm sized Fe₂O₃ particles under 1.2 MHz magnetic field. Since then, there have been numerous publications describing a variety of schemes using different types of magnetic materials, different field strengths and particles⁶⁻¹¹. The principle of hyperthermia is that cancer cells are much more sensitive to and intolerant of the effects of excessive heat than normal cells. Also, tumours have an impaired ability to adapt their blood circulation to the effects

of high temperatures and thus hyperthermia can cause a reduction of blood flow to a tumour. The application of magnetite nanoparticles (NPs) to hyperthermia treatment requires the homogenous dispersion of magnetite nanoparticles in human body fluid. To understand the dispersion of magnetite nanoparticles, we synthesized different-sized nanoparticles and try to modify the surface to confer hydrophilicity.

EXPERIMENTAL

Synthesis of magnetite nanoparticles with iron(III) acetylacetonate concentration: 1, 2, 3 and 4 mmol of iron(III) acetylacetonate [Fe(acac)₃, Aldrich Chemical] was dissolved into 20 mL benzyl ether and 10 mmol of 1,2 hexadecanediol, 6 mmol of oleic acid and its equivalent mole of oleyl amine were added. The key to successful synthesis of monodisperse magnetite nanoparticles is preheating the solution at 200 °C for 2 h and then refluxing at 300 °C for 1 h under nitrogen gas flow (Fig. 1)^{12,13}. Polyols like 1,2-hexadecanediol in this paper are more polar and form stronger associates with metal ions; chelating agents for metal ions to form metal complexes. Oleic acid is a capping ligand as a stabilizing agent. Iron chloride or nitrate reacts with oleic acid to form iron oleate. The thermal decomposition of the iron oleate is already studied to synthesize

†Presented at The 7th International Conference on Multi-functional Materials and Applications, held on 22-24 November 2013, Anhui University of Science & Technology, Huainan, Anhui Province, P.R. China

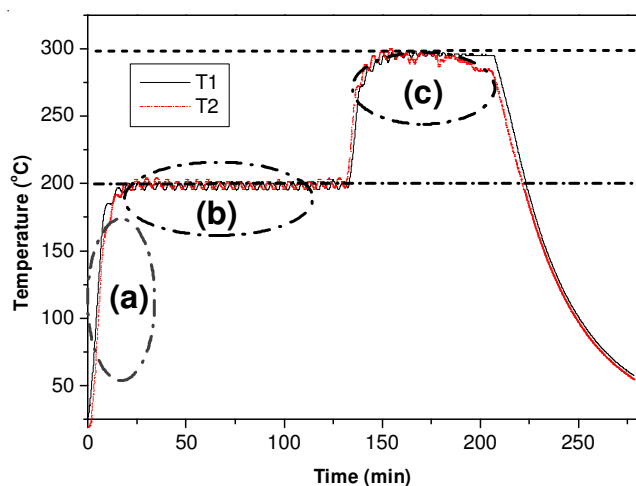
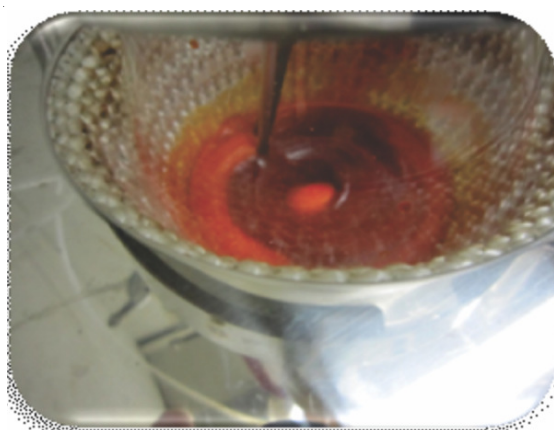


Fig. 1. Magnetite synthesis photograph (left) and temperature profile for the synthesis of magnetite nanoparticles by thermal decomposition method. Dissolution stage (a), nucleation stage (b) and crystal growth stage during reflux for 1 h (c)

magnetite nanoparticles^{12,13}. In this study, we fixed 20 mL benzyl ether as a solvent and 6 mmol of oleic acid and equivalent molar concentration of oleyl amine were used as stabilizing agents and 1,2-hexadecanediol was used as a complexing agent. The aim of our study is focused on the synthesis of magnetite nanoparticles according to precursor or stabilizing agents. We chose a thermal decomposition method for the synthesis of magnetite nanoparticles. To separate magnetite nanoparticles, we centrifugated the refluxed solution at 20,000 rpm for 10 min and washed 3 times with ethanol and obtained oleic acid capped magnetite nanoparticles. The molar concentration of iron acetylacetonate was changed from 40 to 160 mM. Therefore, the molar ratio of $\text{Fe}(\text{acac})_3$ as precursor and oleic acid and oylamine as surfactant were changed to 1:6, 1:3, 1:2 and 2:3 (Table-1).

Surface modification of magnetite nanoparticles with molar concentration: The magnetic nanoparticles in biomedical

application need to be hydrophilic; the hydrophobic Fe_3O_4 colloid in hexane was transformed to hydrophilic Fe_3O_4 nanoparticles using polyethylene glycol (PEG). The solvent hexane was evaporated from the magnetite disperse solution under a flow of nitrogen gas, producing black solid magnetite nanoparticles. The residue was dissolved in chloroform to form the homogeneous dispersion of magnetite at a concentration of 0.5 mg particles/mL solution. 1 mL of chloroform solution of polyethylene glycol (10 mg/mL) was added into 2 mL of the nanoparticle dispersion. The mixture was shaken at 37 °C for 1 h and chloroform was evaporated under nitrogen gas in a vacuum oven for 1 d. (Table-2) The solid residue could be dispersed in phosphate buffered saline (PBS) solution for further test.

TABLE-2
CHEMICAL COMPOSITIONS FOR THE SURFACE
MODIFICATION OF MAGNETITE NANOPARTICLES
(F1-F4) WITH PEG

	F1	F2	F3	F4
Magneties (mg)	27	24	24	23
PEG (mg)	400	400	400	400
Chloroform (mL)	40	40	40	40

Characterization of nanoparticles and coating nanoparticles: The crystal morphologies of magnetite nanoparticles synthesized from different iron acetylacetonate concentrations were observed by transmission electron microscope (TEM; JEM 2000, 200 kV, point-to-point resolution 0.15 nm, JEOL Co., Ltd.). Fourier-transformed infrared (FT-IR, Prestige, Shimadzu, Japan) spectroscopy were also used for the analysis of surface state of magnetite nanoparticles. Thermal decomposition behaviours were also characterized by using differential thermal analysis and thermogravimetric analysis equipment (DTA-TG, Shimadzu DTG50, Japan). For the analyses of FT-IR and DTA-TG, we prepared as-prepared oleic acid capped magnetite nanoparticles, magnetite nanoparticles washed three times with hexane to remove excessive organics and magnetite surface modified with polyethylene glycol.

RESULTS AND DISCUSSION

The crystal morphologies of magnetite nanoparticles synthesized by the thermal decomposition were observed by transmission electron microscope (TEM) (Fig. 2). The crystal morphologies of samples of the F2(a) and F2(b) were observed as round shapes and uniform particles, but the crystal morphologies of samples of F3(c) and F4(d) had a little cubic shape. It is suggested that monodisperse magnetite nanoparticles can be formed *via* nucleation and growth (Fig. 1). In the region of temperature rise (a), no nucleation would occur. The colour of solution slowly changed from red to black at the

TABLE-1
CHEMICAL COMPOSITIONS AND CONDITIONS FOR THE SYNTHESIS OF MAGNETITE NANOPARTICLES

Samples	$\text{Fe}(\text{acac})_3$ (mmol)	Oleic acid (mmol)	Oleyl amine (mmol)	1,2-Hexadecanediol (mmol)	Benzyl ether (mL)	Molar concentration (mM)
F1	1	6	6	10	20	40
F2	2	6	6	10	20	80
F3	3	6	6	10	20	120
F4	4	6	6	10	20	160

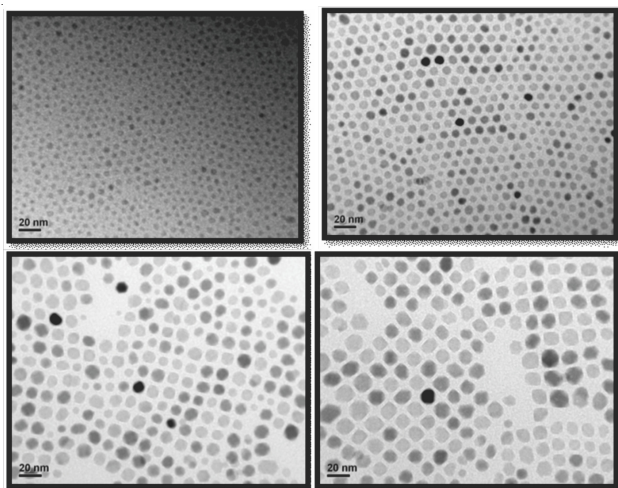


Fig. 2. TEM images of as-prepared magnetite nanoparticles ($\times 200$ k) with molar concentration, F1 (a), F2 (b), F3 (c), F4 (d) and their magnified images ($\times 500$ k) of magnetite nanoparticles samples, F1 (e), F2 (f), F3 (g), F4 (h), respectively

temperature increase step. The nucleation occurs only when the supersaturation reaches a certain value above the solubility [(b)], which corresponds to nucleation temperature to override the energy barrier for the formation of nuclei. When the

concentration decreases below this specific saturation concentration, which corresponds to the critical E, no more nuclei would form, whereas the growth proceeds until the concentration of growth species has attained the equilibrium concentration or solubility [(c)]. In our experiment, it is found that the crystal sizes increased with the molar concentration of iron acetylacetonate. The distributions of crystal sizes were shown in Fig. 3. It was 4 nm for F1 of 40 mM, 7 nm for 80 mM, 10 nm for 120 mM and 12 nm for 160 mM. The crystal sizes are dependent on the concentration of iron ions. In the solution, nucleation occurs by forming nuclei, aggregations of iron ions. The crystals begin to grow, when the nuclei is stable thermodynamically over critical size. During reflux at 300 °C, magnetite nanocrystals are produced. We can control the crystal size between 4 and 12 nm in the range of 40 and 160 mM of concentration.

However, it is more valuable to understand the behaviour of secondary particle size of magnetite in the solution, because nanoparticles naturally aggregate themselves in the solvent to decrease the thermodynamic and electrostatic energy. In our experiment, we dispersed oleic acid-capped magnetite nanoparticles in normal hexane and measured the secondary particles by Mie's scattering particle size analysis method. The distributions of the secondary particle size are shown in Fig. 4.

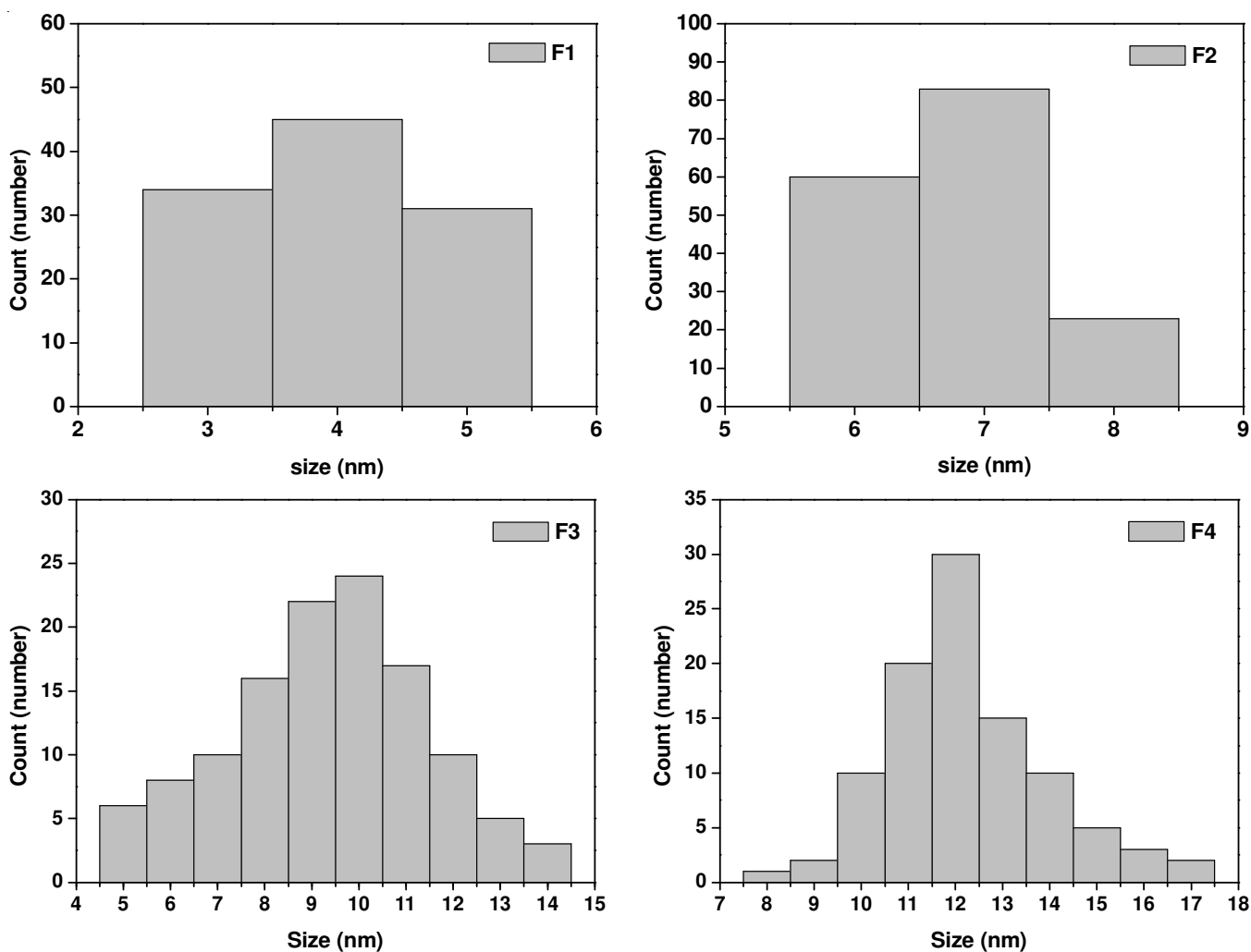


Fig. 3. Primary particles size distributions of magnetite nanoparticles of F1 (a), F2 (b), F3 (c) and F4 (d)

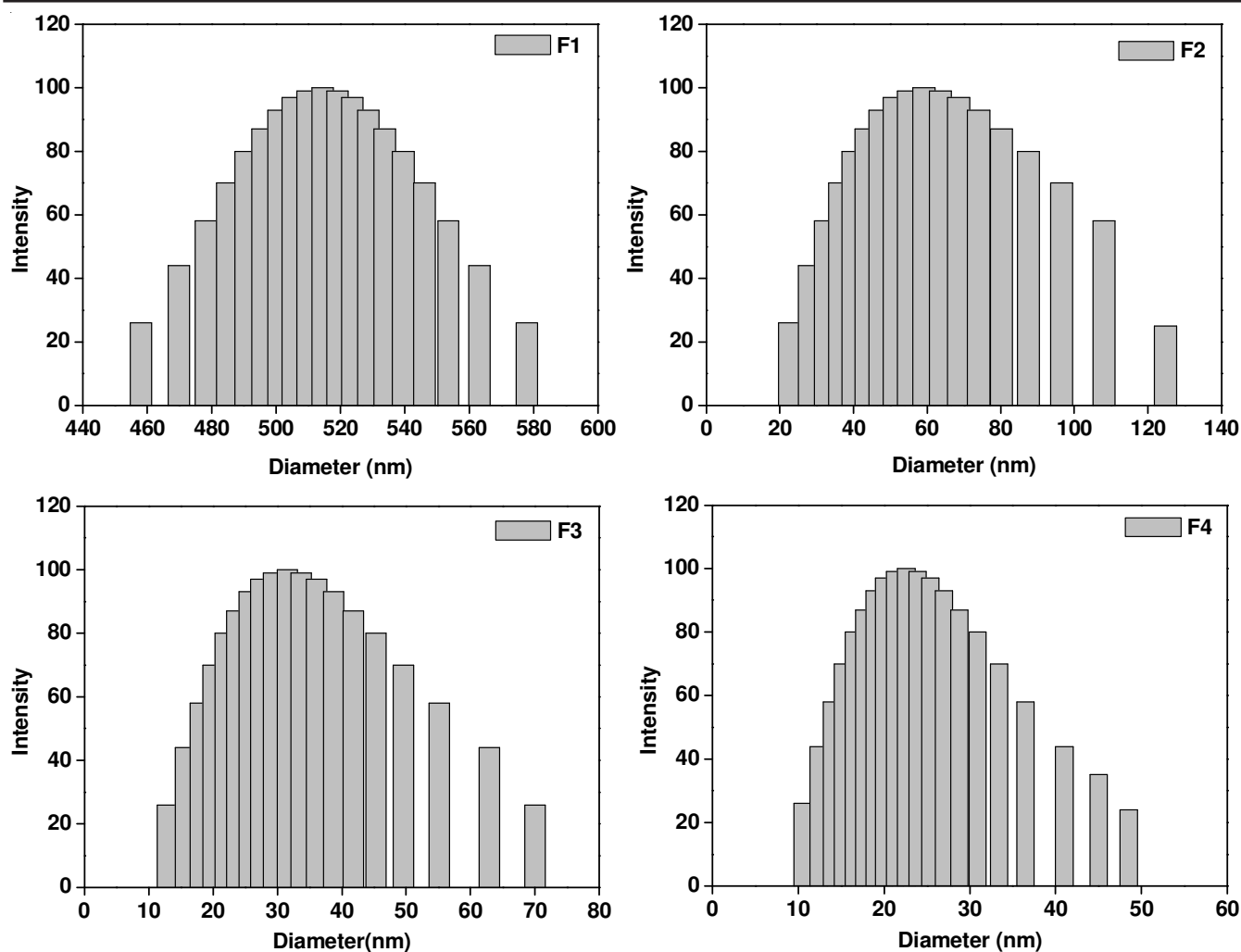


Fig. 4. Size distributions of magnetite nanoparticles of F1 (a), F2 (b), F3 (c) and F4 (d), respectively. The particle size distributions were measured by laser particle size analyzer. The magnetite nanoparticles were dispersed in organic solvent hexane

The average values of F1, F2, F3 and F4 were roughly 520, 60, 35 and 25 nm. It shows that the smaller primary particles tend to form the larger secondary particles. Normally, the surface charges and energies of the smaller particles are known to be larger, so that the smaller particles tend to aggregate themselves to form the larger secondary particles. In this result, we know that the smaller particles tend to aggregate more easily and it is difficult to disperse the smaller particles homogeneously. Therefore, we can say that the most optimum primary particle size is 20-25 nm in the viewpoint of dispersion.

Magnetite nanoparticles are encapped with oleic acid when we synthesize the magnetite *via* thermal decomposition method using oleic acid and oleyl amine as stabilizing agents. The product of magnetite is composed of magnetite nanoparticles and oleic acid. To analyze the amount of oleic acid and magnetite, we characterized the thermal behaviour of the obtained products *via* DTA and TG method. Thermal curves show the thermal behaviour of as-prepared magnetite nanoparticles encapped with oleic acid and the thermal behaviour of washed magnetite nanoparticles are analyzed. As-prepared magnetite nanoparticles are comprised of 90-97 % of oleic acid or organic elements and 3-10 % of magnetite solid contents. The removal of organics occurred *via* various steps from DTA analysis results. At around 200 °C, the endothermic peak might

be related with the evaporation of solvent benzyl ether. We observed three endothermic peaks between 300 and 500 °C, which are considered to be removal of oleyl amine, oleic acid or remaining organics. After washing, the products are comprised of 75-85 % of solid magnetite nanoparticles. It is known that washing away of organics from F1 samples is more difficult than F2, F3 and F4 samples. It is inferred that the difficult washing away from the smaller particles are related with surface area.

TG-DTA results of the as prepared nanoparticles with molar concentration, F1 (a), F2 (b), F3 (c), F4 (d). F1 exhibited weight loss in the temperature range 200-400 °C. The weight loss began at 200 °C and the three major reductions due to the decomposition of oleic acid, benzyl ether and oleylamine, these boiling points are 195, 298 and 350 °C, respectively. The weight loss at the initial stages was caused by the evaporation of the residual oleic acid. The remaining solid contents after decomposition, F1, F2, F3 and F4 were 10, 5, 5 and 3 %, respectively. However, after washing several times, F1, F2, F3 and F4 were 74.4, 84, 84.5 and 87 %, respectively. The better washing the solvent and organic materials well.

FT-IR spectra show the surface encapping states of magnetite nanoparticles in the steps of as-prepared and after washing and surface modification with polyethylene glycol

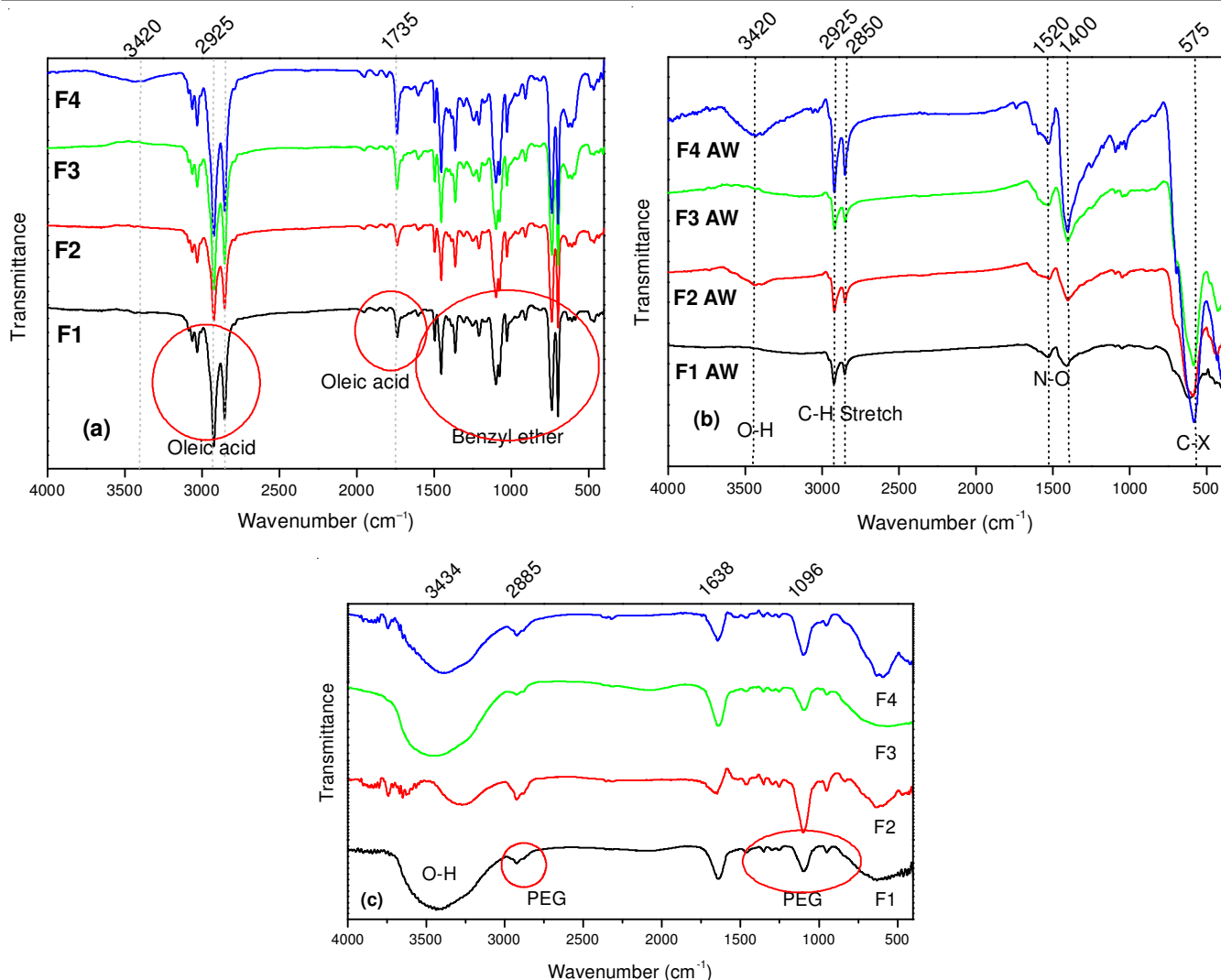


Fig. 5. FT-IR spectra of magnetite nanoparticles with molar concentration. (a) as-prepared, (b) after washing and (c) PEG-modified state

(Fig. 5). As-prepared magnetite nanoparticles showed CH and CO peaks of oleic acid at 2925 and 1735 cm^{-1} and peaks of benzyl ether around 1500 cm^{-1} . It indicates that as-prepared magnetite nanoparticles are comprised of organic solvent, encapping agents and solid magnetite elements. After washing, most of solvent and encapping agents are removed from FT-IR analysis spectra in Fig. 5(b). However, the surface is known to be encapped with CH and CO. The surface shows the hydrophobicity. To disperse the magnetite in water-based solvent like human body fluid, the surface was modified with polyethylene glycol. After the surface modification, we found the appearance of OH vibration and bending mode at around 3400

and 1630 cm^{-1} . This means that hydroxylation of magnetite surface was performed *via* the reaction of polyethylene glycol and CH and CO-encapped surface of magnetite. The surface has the property of hydrophilicity and easy dispersability in water.

Properties of magnetite with control of crystal sizes and surface modified states for hyperthermia application were summarized in Table-3. Magnetite nanoparticles with 11 nm of primary size showed the best properties, 61 emu/g of saturated magnetization and maximum temperature of 54 $^{\circ}\text{C}$ from initial temperature 22 $^{\circ}\text{C}$ under AC magnetic field for 1 h of irradiation.

TABLE-3
PROPERTIES OF DIFFERENT MAGNETITE NANOPARTICLES SYNTHESIZED FROM DIFFERENT MOLAR CONCENTRATIONS

Items	F1	F2	F3	F4
Primary size (nm)	4	7	9	11
Secondary size (nm)	514.5	59.1	31.5	22.6
Yield (%)	53	77	86	91
Solid contents	As-prepared nanoparticles (%)	10	5	3
	Nanoparticles after washing (%)	74.4	84	87
	Ms (emu/g)	40.7	53	58.7
Hyperthermia	Max. temp. ($^{\circ}\text{C}$)	49	51	54
	Temp. increase ($^{\circ}\text{C}$)	27	30	33

Conclusion

The homogeneous dispersion of magnetite is sufficient and necessary condition for their bioapplication. In this paper, we synthesized different-sized magnetite nanoparticles between 4 and 12 nm *via* thermal decomposition of iron acetylacetonate. In the viewpoint of aggregation, the larger sized magnetite is more homogeneously dispersed from the results of secondary particle size analysis. The surface modification and control of hydrophilicity is very important, because magnetite nanoparticles are used in our human body. The homogeneous dispersion in human body fluid requires the hydrophilic surface. For this, we could modify the surface to be hydrophilic *via* polyethylene glycol reaction. We suggest the magnetite nanoparticles with around 25 nm sizes and their surface modified with polyethylene glycol could be homogeneously dispersed in human body.

ACKNOWLEDGEMENTS

The authors are appreciated for the financial support of Korea Ministry of Knowledge and Economy, the core material research and development program.

REFERENCES

1. M.H. Seegenschmied and C.C. Vernon, in eds.: M.H. Seegenschmied, P. Fessenden and C.C. Vernon, *A Historical Perspective on Hyperthermia in Oncology. : Thermoradiotherapy and Thermochemotherapy*, Vol. 1, Springer Verlag, Berlin, pp. 3-44 (1995).
2. G.F. Baronzio and E.D. Hager, *Hyperthermia in Cancer Treatment*, Springer, New York, USA (2006).
3. S. Mornet, S. Vasseur, F. Grasset and E. Duguet, *J. Mater. Chem.*, **14**, 2161 (2004).
4. M. Johannsen, B. Thiesen, A. Jordan, K. Taymoorian, U. Gneveckow, N. Waldöfner, R. Scholz, M. Koch, M. Lein, K. Jung and S.A. Loening, *Prostate*, **64**, 283 (2005).
5. R.K. Gilchrist, R. Medal, W.D. Shorey, R.C. Hanselman, J.C. Parrot and C.B. Taylor, *Ann. Surg.*, **146**, 596 (1957).
6. M. Shinkai, M. Yanase, M. Suzuki, H. Honda, T. Wakabayashi, J. Yoshida and T. Kobayashi, *J. Magn. Magn. Mater.*, **194**, 176 (1999).
7. A. Jordan, R. Scholz, P. Wust, H. Fahng and R. Feliz, *J. Magn. Magn. Mater.*, **201**, 413 (1999).
8. T. Minamimura, H. Sato, S. Kasaoka, T. Saito, S. Ishizawa, S. Takemori, E. Tazawa and E. Tsukada, *Int. J. Oncol.*, **16**, 1153 (2000).
9. P. Moroz, S.K. Jones, J. Winter and A.N. Gray, *J. Surg. Oncol.*, **78**, 22 (2001).
10. S.K. Jones, J.W. Winter and A.N. Gray, *Int. J. Hyperthermia*, **18**, 117 (2002).
11. I. Hilger, K. Frühauf, W. Andrä, R. Hiergeist, R. Hergt and W.A. Kaiser, *Acad. Radiol.*, **9**, 198 (2002).
12. J. Park, K. An, Y. Hwang, J.-G. Park, H.-J. Noh, J.-Y. Kim, J.-H. Park, N.-M. Hwang and T. Hyeon, *Nat. Mater.*, **3**, 891 (2004).
13. S. Sun and H. Zeng, *J. Am. Chem. Soc.*, **124**, 8204 (2002).